Monitoring the Evolution of the X-ray Remnant of SN 1987A

Sangwook Park, David N. Burrows, Gordon P. Garmire, and John A. Nousek

Department of Astronomy and Astrophysics, Pennsylvania State University, 525 Davey
Laboratory, University Park, PA. 16802

and

Richard McCray, Eli Michael, and Svetozar Zhekov

Joint Institute for Laboratory Astrophysics, University of Colorado, Campus Box 440,
Boulder, CO. 80309-0440

ABSTRACT

We report on the results of our monitoring program of the remnant of SN 1987A with the Advanced CCD Imaging Spectrometer (ACIS) on board the *Chandra X-ray Observatory.* Two new observations have been performed in AO2, bringing the total to four monitoring observations over the past two years. Over this time period, new techniques for correction of "Charge Transfer Inefficiency (CTI)" and for use of charge spreading to provide angular resolution somewhat better than the pixel size of the CCD detector have become available at Penn State. We have processed all four observations using sub-pixel resolution to obtain the highest possible angular resolution, and using our CTI correction software to provide more reliable spectral analysis and flux estimations.

The high angular resolution images indicate that the X-ray bright knots are convincingly correlated with the optical spots, primarily at $\lesssim 1$ keV, while higher energy photons are very well correlated with radio images. Our data also provide marginal evidence for radial expansion of the X-ray remnant at a rate of 5200 $\pm$ 2100 km s^{-1}. The X-ray flux appears to linearly increase by $\sim 60\%$ over the 18 month period of these observations. The spectrum is dominated by broad complexes of atomic emission lines and can be fit with a simple model of a plane-parallel shock with electron temperatures of $kT \sim 2 - 4$ keV and a postshock electron density of $n_e \sim 210 - 420$ cm^{-3}. The implied $0.5 - 10$ keV band luminosity in 2001 April is $\sim 1.3 \times 10^{35}$ ergs s^{-1}; as of that date, we still observe no direct evidence for the central point source, with an upper limit on the *observed* luminosity of $L_X \sim 5.5 \times 10^{33}$ ergs s^{-1} in the $2 - 10$ keV band.

Subject headings: supernovae: general — supernovae: individual (SN 1987A) — supernova remnants — X-rays: general — X-rays: stars

1. INTRODUCTION

With a known age (the supernova explosion in 1987; Shelton et al. 1987), distance ($\sim$50 kpc in the Large Magellanic Cloud [LMC]; Andreani et al. 1987), and progenitor (Sanduleak $-69°202$, a type B3 I star) (Kirshner et al. 1987; Sonneborn et al. 1987), SN 1987A provides a very rare yet excellent astrophysical laboratory for the study of the evolution of a supernova remnant (SNR) in the early phase. The supernova explosion for SN 1987A has also confirmed core collapse in Type II SN by the detection of a neutrino burst (Koshiba et al. 1987). Since its discovery, SN 1987A has thus been intensively studied with space-borne and ground-based instruments over the entire electromagnetic spectrum (e.g., Chevalier 1992 and references therein).

Optical observations with the *Hubble Space Telescope* (HST) have shown an elliptical inner ring around the remnant as well as two closed outer loops (Burrows et al. 1995). The inner ring is believed to be a result of the interactions of the stellar winds from two phases of the progenitor (Luo & McCray 1991; Wang & Mazzali 1992; Blondin & Lundqvist 1993). Inside of this ring is an HII region produced by the UV radiation from the progenitor star (Chevalier & Dwarkadas 1995), with rapidly expanding ejecta clearly visible at the center of *HST* images. The broad high-velocity (4000 km s^{-1} $-$ 15000 km s^{-1}) Lyα and Hα emission detected with the *HST* Space Telescope Imaging Spectrograph (STIS) comes from a reverse shock located at $\sim$75% of the inner ring radius (Michael et al. 1998), which is propagating into the ejecta. The *HST* data have also exhibited the emergence of several "optical spots" along the inner ring since the first detection of such an optically bright spot in 1997 (Pun et al. 1997; Garnavich et al. 1997). These optically brightening spots are interpreted as the emission by radiative shocks as the supernova blast wave begins to strike inward protrusions of the dense material ($n \sim 10^4$ cm^{-3}) in the inner ring (Michael et al. 2000; Michael 2000; Pun et al. 2001). The continuing developments

of the optical spots (Lawrence et al. 2000; Bouchet et al. 2000; Maran et al. 2000; Garnavich et al. 2000) thus signal the precursor of an exciting event: a predicted dramatic brightening (up to the 3 orders of magnitudes) of the remnant at almost all wavelengths (Luo et al. 1994; Borkowski et al. 1997a) in the near future as the shock front hits the ring proper.

The X-ray emission from SN 1987A was detected with *ROSAT* and the X-ray lightcurve revealed a steady increase of the soft X-ray flux over the 4-year *ROSAT* observation period (Hasinger et al. 1996). The *ROSAT* observations, however, were unable to resolve the X-ray remnant due to its limited angular resolution ($\sim 5''$), or to determine the nature of the emission due to the low spectral resolution of the PSPC (Hasinger et al. 1996).

Recently, unprecedented high-angular resolution images from observations of SN 1987A with the *Chandra X-ray Observatory* have revealed a shell-like structure of the X-ray remnant which appears to peak just inside of the optical inner ring (Burrows et al. 2000) (B00 hereafter). The size of the shell structure is $1.''2 \times 1.''0$ and the X-ray bright "knots" are roughly associated with the optical spots within uncertainties of $\sim 0.''1$. The $0.5 - 2$ keV X-ray lightcurve is now increasing much more rapidly than the linear extrapolation of the *ROSAT* lightcurve. The high-resolution dispersed spectrum is dominated by highly ionized atomic line emissions (B00), indicating a thermal origin of the X-ray emission. The implied electron temperature was $kT \sim 3$ keV.

In 2000 December and 2001 April, two new *Chandra* observations of SN 1987A have been performed for the purpose of monitoring the development of the X-ray remnant and we here report the results of the image and the preliminary spectral analysis. The observations are described in §2. The analysis and results are presented in §3 and the implications are discussed in §4. A summary and the conclusions are presented in §5.

2.   OBSERVATIONS & DATA REDUCTION

As part of a monitoring program of SN 1987A, we have performed a total of four observations with the Advanced CCD Imaging Spectrometer (ACIS) on board the *Chandra X-ray Observatory* (Weisskopf et al. 1996) between 1999 and 2001 (Table 1). The first two observations were carried out in 1999 October and 2000 January as a part of the *Chandra* Guaranteed Time Observation (GTO) program. The first observation was taken using the High-Energy Transmission Grating (HETG) and the ACIS-S detector array. The second observation used the ACIS-S3 detector without grating. The detailed description of the observations and some preliminary results have been presented in B00. Two subsequent observations have been made in 2000 December and 2001 April during the AO2 cycle with the same configuration as the second observation.

Over the past two years, the data reduction techniques developed at Penn State have expanded to include new methods for correcting the spatial and spectral degradation of the ACIS data caused by the radiation damage, known as Charge Transfer Inefficiency (CTI) (Townsley et al. 2000; Townsley et al. 2001a), and the use of charge spreading to obtain angular resolution at the sub-pixel level (Tsunemi et al. 2001). The expected effects of the CTI correction include an increase of the number of detected events and improved event energies and the energy resolution (Townsley et al. 2000; Townsley et al. 2001a). By applying the "sub-pixel resolution" method, we expect the angular resolution to improve by ∼10% (Mori et al. 2001). Since the preliminary results from the first two GTO observations as reported in B00 did not incorporate the new data processing, we have reprocessed them for consistency with the third and fourth observations.

We screened all four data sets with the flight timeline filter and turned off the pixel randomization for the highest possible angular resolution. The CTI correction was then applied before further data screenings by status, grade, and the energy selections. The

"flaring" pixels were removed and the *ASCA* grades (02346) were selected. Photons between 0.3 keV and 8.0 keV were extracted for data analysis. The lightcurves around the source regions were examined for possible contamination from variable background emission and no severe variability was found. The typical pileup fraction was small ($\lesssim 4\%$) and can be ignored. After applying these reduction steps, the effective exposures are 116 ks, 9 ks, 99 ks, and 18 ks for the four observations. We then applied the sub-pixel resolution method to improve the angular resolution of the images. The source position of RA = 05^h 35^m $27^s.97$, Dec = $-69°$ $16'$ $11''.09$, based on *Hipparcos* and VLBI data (Reynolds et al. 1995), was used to register the images, and a circular region with a $2''$ radius was used for the extraction of the source spectrum. The total source counts are 690, 607, 9031, and 1800 counts for observations 1, 2, 3, and 4, respectively.

The observed angular size of the SN 1987A remnant in the optical and radio bands is only about $1''.5$ and the ACIS detector pixel size ($0''.492$) is not adequate to resolve the remnant. Fortunately, the intentional "dithering" of the detector array on the sky moves the supernova image across the detector pixels, allowing us to improve the effective resolution by deconvolution techniques. We thus apply a maximum likelihood algorithm (Richardson 1972; Lucy 1974) as described in B00, using $0''.125$ sky pixels (except for the third image, where the improved photon statistics allows us to use $0''.0625$ pixels for the deconvolution). Since the dynamic range in the detected number of photons of our data ($\sim 600 - \sim 9000$ among the four observations) is large, we made a simple test of the reliability of the deconvolved images by deconvolving subsets of the third observation with different numbers of photons in the image deconvolution process. The deconvolved subset images are consistent with the deconvolved full image for subsets including ~ 400 or more counts. We thus conclude that all of our four images are fairly reliable down to an angular resolution of $\sim 0''.1$. The difference in the appearance of the bright spots in the first image compared to those in the other three can be attributed to spectral differences between the

spots and to the fact that the instrument response for the first image is quite different than the response for the last three due to the insertion of the HETG in the beam for the first image only.

The absolute astrometry of the raw data has improved since the first two observations. However, comparisons of the four X-ray images with the *HST* images indicate that there appear to be slight aspect errors among the *Chandra* observations at the level of $\sim 0.''1$. Because of the small angular size of the SN 1987A remnant ($\gtrsim 1''$), this level of uncertainty in the astrometry is still significant and we had to adjust it by hand to obtain the best agreement between the overall X-ray and optical images. The final images are smoothed with $\sim 0.''1$ FWHM for the presentation in Figure 1.

3. ANALYSIS & RESULTS

3.1. X-ray Images

The four X-ray images are presented in Figure 1, overlaid with contours of the *HST* Hα images. Two new *HST* images (taken in 2000 November and 2001 April) have been kindly provided by Peter Challis and the SINS collaboration and these new images are overlaid on the third and the fourth *Chandra* images, respectively. For the first and the second *Chandra* images, we use the *HST* image taken on 2000 February.

As reported in B00, the X-ray remnant has a shell-like morphology with an overall brightening in the eastern half of $\sim 20\% - 30\%$ compared with the western half. The brightest X-ray "knots" in the eastern half are generally correlated with the optical spots as observed with *HST*.

In order to investigate the energy-dependence of the X-ray morphology, we have divided the X-ray images into three broad subbands: the soft band ($0.3 - 0.8$ keV), the mid band

$(0.8 - 1.2$ keV), and the hard band $(1.2 - 8.0$ keV). These three subbands are intended to include the Oxygen line features at $0.6 - 0.7$ keV (soft band), Ne line at $0.9 - 1$ keV (mid band), and Mg and Si lines in the $1.3 - 2$ keV (hard band) (see §3.2) as well as containing relatively equal number of photons ($\sim$one-third of the total counts in each subband). Due to the limited number of photons, reliable subband images are only available for the third and the fourth observations. In Figure 2 the subband images for the third observation are displayed; each subband image contains $\sim$3000 counts. The pixel size in these images is $0\rlap{.}''0625$.

Figure 2 shows that the X-ray peaks in the soft and mid band images are well correlated with the optical spots. Optical Spot 1 at the north-east of the optical inner ring (position angle 29°; Michael et al. 2000) is seen as a bright X-ray knot. Optical Spots $2 - 4$ at the south-east (position angles 91° $-$ 106°; Lawrence et al. 2000) are also X-ray brightened. In the western half, although the overall X-ray brightness is lower than the east, the relatively bright X-ray emission in the south-west may also be associated with an optical spot (spot 6 at position angle 230°; Lawrence et al. 2000). On the other hand, the hard band image, which is *not* well correlated with the optical spots, agrees very well with the structure seen in the radio images as observed with the Australian Telescope Compact Array (ATCA) at 8 GHz. The hard band X-ray image peaks at around the mid-points of the eastern and the western shells (position angles at $\sim$90° and $\sim$270°) (Figure 2d).

Considering the rapid propagation of the supernova blast wave and the $\sim$18 month separation between the first and the fourth observations, we investigate the possibility of detecting the radial expansion of the X-ray remnant. Given the blast wave velocity (~ 4000 km s^{-1}) inferred by the hydrodynamic models (Borkowski et al. 1997b), we expect the diameter of the remnant to change by less than $0\rlap{.}''1$, and such changes will not be apparent to even a detailed direct examination of the images. However, we can increase

our sensitivity to such effects by averaging over the entire remnant using radial profiles. In this way we may lose some detailed information such as the inclination of the ring to the line of sight and individual discrete features, if any, but we can make a statistically more reliable comparison for the overall averaged remnant size. In Figure 3a, radial profiles for the four observations are displayed. Each bin represents the X-ray intensity from a $0.''125$ width annular region centered on the adopted source position. The peak bin is at a radius of $\sim 0.''63$ for all four observations. The brightness at the radius of $\sim 0.''75$ however appears continuously increasing while the intensity at $\sim 0.''50$ bin decreases such that the mean radius of the shell moves measurably outwards with time. In order to accurately quantify this effect, we reconstructed the radial profiles centered on the mean position of the count distribution (or "center of mass") with a smaller bin ($0.''05$ annular region). We then fit these radial profiles with Gaussians and plot the best-fit Gaussian peaks versus time in Figure 3b. The peak radius increases by $\sim 0.''04$ from 1999 October to 2001 April. We tested this estimation with different annular bin sizes of $0.''025$, $0.''05$, and $0.''125$ because such a small change in angular size of $0.''04$ might have been affected by the selected bin size. The results are the same regardless of the selected annular bin sizes. We also compared the averaged angular sizes by simply estimating the mean (or "center of mass") radii among the observations instead of fitting with a Gaussian in case of the existence of any systematic bias with the Gaussian fittings. Regardless of the annular bin sizes, the $\sim 0.''04$ increase in the radius is persistent with this simple estimation as well.

The best-fit expansion rate of the X-ray remnant, indicated by the solid line in Figure 3b, is 5200 ± 2100 km s^{-1}. This expansion rate is in agreement with the rate determined from radio observations (Gaensler et al. 2000), and is also consistent with the *HST* STIS observations of Lyα and Hα (Michael et al. 1998) as well as with the theoretical predictions (Borkowski et al. 1997b). Finally, we measured the radial expansions along the major (east-west) and minor (north-south) axes of the ring in order to probe the effects of

the inclination angle of the ring to the line of sight in the overall expansion estimations. The results appear generally consistent with the overall expansion: i.e., the radial expansion is $\sim0.''03$ along both directions of the major and minor axes. The slight difference in the expansion rate between the major and minor axis directions is statistically insignificant.

3.2.   Spectrum & Lightcurve

The undispersed spectra of SN 1987A from all four *Chandra* observations are presented in Figure 4. Each spectrum has been rebinned to provide a minimum of 20 counts per bin. The energy range of $0.5 - 4.0$ keV (which typically contains $\gtrsim90\%$ of the total counts) is used for the spectral fitting. For the spectral analysis of our CTI corrected data, we have utilized the response matrices appropriate for the spectral redistribution of the CCD, as generated at Penn State (Townsley et al. 2001b). Broad emission line features are evidently present in each observation, supporting a thermal origin of the observed X-ray emission. The broad line profiles correspond to O, Ne, Mg, and Si line complexes as reported in B00 from the dispersed spectrum of the first observation.

The observed spectrum can be described with a plane-parallel shock model with an electron temperature of $kT = 2 - 4$ keV and an average ionization timescale of $nt \sim 8 \times 10^{10}$ cm^{-3} s being absorbed by N$_H \sim 1 \times 10^{21}$ cm^{-2}. The elemental abundances were fixed for H (= 1), He (= 2.57), and C (= 0.09) at the appropriate values for the inner circumstellar ring (Lundqvist & Fransson 1996) and Ca (= 0.34) and Ni (= 0.62) at values for the LMC (Russell & Dopita 1992) (hereafter, all abundances are with respect to the solar) since the contribution from these species in the spectral fitting is expected to be insignificant in the selected energy range. Other elements were allowed to vary and fit the data with sub-solar abundances: e.g., for the 2000-December data, the best-fit abundances are N = 0.01, O = 0.04, Ne = 0.12, Mg = 0.08, Si = 0.24, S = 0.40, and Fe = 0.07. Our

simple model consistently fits all four data sets with moderately acceptable statistics ($\chi^2_\nu = 1.2 - 1.6$).

With this simple model, the $0.5 - 2.0$ keV band X-ray fluxes of SN 1987A for our four observations are $\sim 1.5 \times 10^{-13}$ ergs s^{-1} cm^{-2}, $\sim 1.6 \times 10^{-13}$ ergs s^{-1} cm^{-2}, $\sim 2.2 \times 10^{-13}$ ergs s^{-1} cm^{-2}, and $\sim 2.4 \times 10^{-13}$ egrs s^{-1} cm^{-2}. (The X-ray fluxes for the first and the second observations have been recalculated using our current processing with CTI correction, and the revised fluxes increased by $\sim 15\%$ from those presented in B00.) Based on these flux estimations, the long-term X-ray lightcurve of SN 1987A is presented in Figure 5. In Figure 5a, an updated long-term radio flux variation (Manchester et al. 2001) is presented for comparison. For the X-ray lightcuve, the $ROSAT$ fluxes were taken from Hasinger et al. (1996) and have been converted for comparison with the ACIS data as presented in B00 (Figure 5b). The $0.5 - 2.0$ keV X-ray flux and luminosity between 1999 and 2001 are listed in Table 2.

The X-ray flux has been increasing at a constant rate for the past 18 months, and is now brightening much faster than expected from the linear extrapolation of the $ROSAT$ lightcurve. We note that the interpolated date of this slope change in the lightcurve, for both the X-ray and radio data, is about 1997, when the first optical spot was discovered. The net increase in the X-ray flux between 1999 October and 2001 April is $\sim 60\%$. Assuming a distance of 50 kpc, and correcting for the interstellar absorbing column of 10^{21} cm^{-2} inferred from our spectral fits, the $0.5 - 2$ keV X-ray luminosity was $\sim 0.7 \times 10^{35}$ ergs s^{-1} ($\sim 1.0 \times 10^{35}$ ergs s^{-1}, in the $0.5 - 10$ keV band) in 1999 October and was $\sim 1.0 \times 10^{35}$ ergs s^{-1} ($\sim 1.3 \times 10^{35}$ ergs s^{-1}, in the $0.5 - 10$ keV band) in 2001 April.

Assuming a spherical shell for the X-ray emitting volume, the best-fit emission measure for the 2000-December observation implies a postshock electron density of n_e ~ 210 cm^{-3} to ~ 420 cm^{-3}. In this estimation, we have assumed a spherical shell of an

inner radius of $0''.6$ (Gaensler et al. 2000) and a range of the outer radius of $0''.7 - 0''.9$ (from our data) for the X-ray emitting volume. We also assumed $n_e \sim 1.5 n_H$ for the ring abundances (e.g., Masai & Nomoto 1994). Considering our simple modeling and the embedded uncertainty in the assumed geometry, the derived range of the electron density is in good agreement with the previously suggested values for the preshock HII region (Chevalier & Dwarkadas 1995; Borkowski et al. 1997b; Lundqvist 1999), assuming density enhancement by a factor of 4 at the front of a strong adiabatic shock.

4. DISCUSSION

The overall appearance of the X-ray images of SN 1987A shows little change over the one and a half year observation period: i.e., the shell-like overall morphology, brighter emission in the eastern half, and the general correlations of the X-ray brightening with the optical spots. (The most noticeable difference is the supression of Spot 1 in our first observation, which we believe to be due to lower sensitivity to this soft feature, due to the insertion of the HETG into the optical path for this observation.) The correlations of the X-ray peaks with the optical spots in the images of the first and the second observations are generally better than found by B00, which is likely an effect from our improved data processing. The observed shell-like X-ray emission is interpreted as X-ray emission from the shocked SN ejecta and the shocked circumstellar material between the supernova blast wave and the reverse shock (B00 and the references therein). The origin of the overall X-ray brightness asymmetry between the east and the west may be related to the asymmetric distribution of SN ejecta and/or to the density variation of the circumstellar medium. Extensive spectral analyses will be necessary in order to answer this question, which is beyond the scope of the current work.

The comparisons among the images and the radial profiles show evidence of the radial

expansion of the X-ray shell of SN 1987A. We have assumed constant expansion during the 18 month duration of our monitoring observations. Although the blast wave velocity may not be constant in time due to the interaction with the circumstellar material, the quality of the data do not justify more complex fits at this time. The change in the angular radius ($\sim$0$.\!\!''$04) is smaller than the angular resolution of the deconvolved images. Although the peak radius appears to be monotonically increasing, the derived expansion rate is only a 2.5σ result. Considering systematic uncertainties associated with the image processing (e.g., the image deconvolution, the selected source position etc.), we therefore must consider this result to be of marginal significance. Follow up observations will be necessary for more definitive measurements of this interesting aspect of the SNR.

The broad subband images show that the X-ray bright knots in the soft band are well correlated with the optical spots, typically within $\sim$0$.\!\!''$05, while such correlations are not observed in the hard band. Particularly the origin of the bright X-ray emission feature at position angles $\sim$90° and $\sim$270° in the hard band draws our attention. We have investigated the possibility of a coincidental detection of a background extragalactic object. We searched for possible counterparts in 33 multi-wavelength catalogs of galaxies and radio sources available through the HEASARC on-line database and no such candidates were found within 1$'$ radius of our reference source position. We have estimated the "source" flux from the spectrum of the bright hard X-ray knot in the west ring (position angle $\sim$ 270°). The extracted spectrum contains $\sim$400 photons and is best fitted in the $0.5 - 5$ keV band with a power law plus plane-parallel shock model ($\Gamma = 2.1$, $kT = 2$ keV, $nt = 9 \times 10^{10}$ cm^{-3} s, χ^2_ν ~ 1.0). The estimated flux is $\sim$1 $\times$ 10^{-14} ergs s^{-1} cm^{-2} in both of the $0.5 - 2$ keV and the $2 - 10$ keV band, and based on the recent *Chandra* logN-logS relations of the *Hubble Deep Field* (Brandt et al. 2001), the probability of a coincidental detection of an extragalactic source within the angular size of SN 1987A ($\sim$1 arcsec^2) is only $\sim$10^{-5}. The spectral index ($\Gamma = 2.1$) may be in the range of nearby broad line AGNs but clearly deviates from typical

AGNs ($\Gamma \lesssim 1.5$) (Alexander et al. 2001 and references therein). We thus conclude that this hard X-ray spot is emission from the supernova remnant. These bright hard X-ray knots are on the other hand well correlated with the radio emission. This can be understood if the hard X-ray emission and radio emission both originate in the fast shock (~ 4000 km s^{-1}) propagating into the HII region. As this shock hits the denser, neutral ring material, the shock slows down significantly. Soft X-rays are emitted from the leading edge of these knots, with oblique radiative shocks on the sides of the dense knots ($\lesssim 300$ km s^{-1}) providing the correlated optical and UV emission (Michael et al. 2000; Michael 2000; Pun et al. 2001).

A recent result from the observation of SN 1987A with *XMM-Newton Observatory* has suggested a non-thermal component at > 4 keV, which is speculated to be emission from the embedded pulsar and its wind nebula (Aschenbach et al. 2001). Although our spectral analysis did not require a power-law component, the observed correlation between the hard X-ray and radio images may suggest such a contribution. We used the same one temperature plane-parallel shock model, now with the insertion of a power law, in the 0.5 $- 6$ keV band to investigate this possibility. The improvement of the fit after including a power-law component appears statistically significant based on the F-test. The overall fits are however practically indistinguishable, e.g., $\chi^2_\nu = 1.05$ with a power law and $\chi^2_\nu = 1.12$ without a power law, for the purposes of our preliminary spectral analysis. There are small changes in the best-fit electron temperature and the ionization timescale, which are insignificant. The photon index for the best-fit power law ($\Gamma \sim 2.3$) is consistent with the shock-accelerated synchrotron radiation observed with young Galactic supernova remnants (Koyama et al. 1995; Koyama et al. 1997; Keohane et al. 1997; Allen et al. 1997). The inclusion of a power law results in relatively higher elemental abundances, generally at above-solar level compared with the sub-solar abundances without the power-law component. This simple test implies that the presence of a power-law component as a contributor in the observed X-ray spectrum, particularly in the hard band, cannot be

ruled out, although it is not required by our data. The physical origin of the non-thermal emission, if detected at all, is however unclear considering the early phase of the SNR evolution: i.e., it is unlikely from the embedded pulsar or its nebula since we have yet to see such evidence with our high resolution ACIS images (see discussion below), and the age of the SNR may not be old enough to accelerate the particles to hard X-ray energies, although the best-fit photon index is plausible for such origins. The implied high metal abundances with the power-law component suggest the SN ejecta as a dominating source of the X-ray emission, which may also be inappropriate for such an early stage of the SNR as predicted by hydrodynamic models (Borkowski et al. 1997b). We thus defer the issue of the non-thermal contribution in the observed spectrum of SN 1987A to future investigations.

The best-fit parameters for the observed spectrum indicate no significant change from the results in B00. The best-fit electron temperatures are substantially lower than the expected postshock ion temperature for the implied shock velocities, which is not surprising since the time scale to reach an equilibrium between the electron and ion temperatures is much longer than the age of SN 1987A. This non-equilibrium status between the electron and ion temperatures suggests that it may require more complicated treatments in the spectral analysis instead of a simple one temperature plane-parallel shock model as we have utilized in the current work. Due to the limited number of photons, an extensive spectral analysis is feasible only with the third observation and such an analysis is presented in a separate paper (Michael et al. 2001). Michael et al. (2001) demonstrate that the spectrum of SN 1987A can be best described with more complex models rather than the simple model used here.

The X-ray lightcurve demonstrates that the remnant of SN 1987A has been continuously brightening in X-rays over the last $\sim$10 years. Between 1991 and 1995 the $0.5 - 2.0$ keV band X-ray flux was increasing at a rate of $\sim$$2.0 \times 10^{-17}$ ergs s^{-1} cm^{-2} per day ($\chi^2_\nu = 0.1$).

As of 2001 April, the observed intensity of the X-ray remnant has increased by a factor of $\sim$6 since the 1995-November *ROSAT* observation. This is almost 3 times brighter than would be expected from the extrapolations of the flux increase rate with the *ROSAT* observations. The $0.5 - 2.0$ keV X-ray flux is currently increasing at a constant rate of $\sim 1.67 \times 10^{-16}$ ergs s^{-1} cm^{-2} per day ($\chi^2_\nu = 0.5$), which is $\sim$8 times higher rate than it was in 1995. The combined *ROSAT* and *Chandra* data cannot be fitted by a quadratic light curve ($\chi^2_\nu = 6.3$), although suggested on theoretical grounds (Masai & Nomoto 1994; Hasinger et al. 1996) (see dotted line in Figure 5b). A simple power law with an index of 2.8 provides a better fit to the combined lightcurve, but cannot fit the *Chandra* data points ($\chi^2_\nu = 3.5$).

The observed bright X-ray emission near the optical spots and the continuously increasing X-ray flux at a higher rate most likely imply that the supernova blast wave is closely approaching the inner ring and that we may shortly be able to see the dramatic turn-up in the remnant luminosity when the blast wave finally reaches and sweeps through the dense inner ring.

As of 2001 April, we still observe no direct evidence of a point source within the X-ray remnant of SN 1987A. We thus estimated a point source detection limit by performing a Monte Carlo simulation to add a simulated point source at the center of the observed SN 1987A remnant. The simulated point source was generated by convolving point sources of various fluxes with the *Chandra* point spread function with photon statistics. The simulated images (with the point source) were compared with the observed image using a χ^2 test. We have utilized the 2000-December observation for this purpose since the large number of detected photons in this observation would provide the most reliable estimation. Because the ejecta are still expected to be optically thick at soft X-ray energies, we restricted this test to hard X-rays ($E > 2$ keV). The 90% confidence limit on the point source counts is $\sim$13% of the total counts at > 2 keV, which implies an *observed* upper limit of $\sim 5.5 \times$

10^{33} ergs s^{-1} in the $2 - 10$ keV luminosity for any embedded point source. Since we do not know the optical depth of the overlaying ejecta, we cannot place limits directly on the actual X-ray emission from the putative compact object.

5. SUMMARY AND CONCLUSIONS

Using the high angular resolution of the *Chandra X-ray Observatory*, we have resolved the X-ray remnant of SN 1987A in four different observations taken over an 18 month period. The stability of the features lends confidence in our image processing techniques, which produce an effective resolution of $\sim 0\!.''1$. The X-ray flux is increasing ~ 8 times faster now than it was five years ago. Soft X-ray images show good agreement between X-ray and optical bright spots, while hard X-ray images show better correlation with radio images from ATCA. This can be understood in terms of a model in which a fast shock propagating into the circumstellar HII region produces the hard X-ray and radio emission, while slower shocks propagating into the dense inner ring are responsible for the soft X-ray and optical spots. Although we show that the observed X-ray spectrum can be described with a single temperature plane-parallel shock model, a more complex model, that is in general consistent with our simple model presented in this work, provides a more physically plausible fit, as shown by Michael et al. (2001). Finally, we demonstrate that the X-ray images suggest an expansion velocity of 5200 ± 2100 km s^{-1} with marginal significance, in agreement with the radio and optical observations as well as the theoretical models.

REFERENCES

Allen, G. E., Keohane, J. W., Gitthelf, E. V., Petre, R., & Jahoda, K. 1997, ApJ, 487, L97

Alexander, D. M., Brandt, W. N., Hornschemeier, A. E., Garmire, G. P., Schneider, D. P., & Bauer, F. E. 2001, AJ, in press

Andreani, P., Ferlet, R., & Vidal-Madjar, A. 1987, Nature, 326, 770

Aschenbach, B., Hasinger, G. et al. 2001, A&A, Submitted

Blondin, J. M., & Lundqvist, P. 1993, ApJ, 405, 337

Borkowski, K. J., Blondin, J. M., & McCray, R. 1997a, ApJ, 477, 281

Borkowski, K. J., Blondin, J. M., & McCray, R. 1997b, ApJ, 476, L31

Bouchet, P., Lawrence, S., Crotts, A., Sugerman, B., Uglesich, R., & Heathcote, S. 2000, IAUC, 7354

Brandt, W. N. et al. 2001, AJ, in press

Burrows, C. J., Krist, J., Hester, J., Sahai, R., Trauger, J. T., Stapelfeldt, K. R., Gallagher III, J. S., Ballester, G. E., Casertano, S., Clarke, J. T., Crisp, D., Evans, R. W., Griffiths, R. E., Hoessel, J. G., Holtzman, J. A., Mould, J. R., Scowen, P. A., Watson, A. M., & Westphal, J. A. 1995, ApJ, 452, 680

Burrows, D. N., Michael, E., Hwang, U., McCray, R., Chevalier, R. A., Petre, R., Garmire, G. P., Holt, S. S., & Nousek, J. A. 2000, ApJ, 543, L149: B00

Chevalier, R. A. 1992, Nature, 355, 691

Chevalier, R. A., & Dwarkadas, V. V. 1995, ApJ, 452, L45

Gaensler, B. M., Manchester, R. N., Staveley-Smith, L., Wheaton, V., Tzioumis, A. K., Reynolds, J. E., & Kesteven, M. J. 2000, Asymmetrical Planetary Nebulae II: From Origins to Microstructures, ASP Conference Series, Vol. 199. ed. by J. H. Kastner, N. Soker, & S. Rappaport, p. 449

Garnavich, P., Kirshner, R., & Challis, P. 1997, IAUC, 6710

Garnavich, P., Challis, P., & Kirshner, R. 2000, IAUC, 7360

Hasinger, G., Aschenbach, B., & Trümper, J. 1996, A&A, 312, L9

Keohane, J. W., Peter, R., Gotthelf, E. V., Ozaki, M., & Koyama, K. 1997, ApJ, 484, 350

Kirshner, R. P., Sonneborn, G., Crenshaw, D. M., & Nassiopoulos, G. E., 1987, ApJ, 320, 602

Koshiba, M. et al. 1987, IAUC, 4338

Koyama, K., Peter, R., Gotthelf, E. V., Hwang, U., Matsuura, M., Ozaki, M., & Holt, S. S. 1995, Nature, 378, 255

Koyama, K., Kinugasa, K., Matsuzaki, K., Nishiuchi, M., Sugizaki, M., Torii, K., Yamauchi, S., & Aschenbach, B. 1997, PASJ, 49L, 7

Lawrence, S. S., Sugerman, B. E., Bouchet, P., Crotts, A. P. S., Uglesich, R., & Heathcote, S. 2000, ApJ, 537, L126

Lucy, L. B. 1974, AJ, 79, 745

Lundqvist, P., & Fransson, C. 1996, ApJ, 464, 924

Lundqvist, P. 1999, ApJ, 511, 389

Luo, D. & McCray, R. 1991, ApJ, 379, 659

Luo, D., McCray, R., & Slavin, J. 1994, ApJ, 430, 264

Maran, S., Pun, C. S. J., & Sonneborn, G. 2000, IAUC, 7359

Masai, K., & Nomoto, K. 1994, ApJ, 424, 924

Manchester, R. et al. 2001, PASA, Submitted

Michael, E., McCray, R., Pun, C. S. J., Borkowski, K., Garnavich, P., Challis, P., Kirshner, R. P., Chevalier, R., Filippenko, A. V., Fransson, C., Panagia, N., Phillips, M., Schmidt, B., Suntzeff, N., & Wheeler, J. C. 1998, ApJ, 509, L117

Michael, E., McCray, R., Pun, C. S. J., Garnavich, P., Challis, P., Kirshner, R. P., Raymond, J., Borkowski, K., Chevalier, R., Filippenko, A. V., Fransson, C., Lundqvist, P., Panagia, N., Phillips, M. M., Sonneborn, G., Suntzeff, N. B., Wang, L., & Wheeler, J. C. 2000, ApJ, 542, L53

Michael, E. 2000, ApJS, 127, 429

Michael, E. et al. 2001, ApJ, Submitted

Mori, K., Tsunemi, H., Miyata, E., Baluta, C. J., Burrows, D. N., Garmire, G. P., & Chartas, G. 2001, "New Century of X-ray Astronomy", March 6 − 8, 2001, Yokohama, Japan

Pun, C. S. J., Sonneborn, G., Bowers, C., Gull, T., Heap, S., Kimble, R., Maran, S., & Woodgate, B. 1997, IAUC, 6665

Pun, C. S. J., Michael, E., Zhekov, S. A., McCray, R. et al. 2001, ApJ, Submitted

Reynolds, J. E. et al. 1995, A&A, 304, 116

Richardson, W. H., 1972, J. Opt. Soc. Am., 62, 55

Russell, S. C. & Dopita, M. A. 1992, ApJ, 384, 508

Shelton, I. 1987, IAUC, 4316

Sonneborn, G., Altner, B., & Kirshner, R. P. 1987, ApJ, 323, L35

Townsley, L. K., Broos, P. S., Garmire, G. P., & Nousek, J. A. 2000, ApJ, 534, L139

Townsley, L. K., Broos, P. S., Nousek, J. A., & Garmire, G. P. 2001a, Nuclear Instruments
        & Methods in Physics Research Section A, in press

Townsley, L. K., Broos, P. S., Chartas, G., Moskalenko, E., Nousek, J. A., & Pavlov, G. G.
        2001b, Nuclear Instruments & Methods in Physics Research Section A, in press

Tsunemi, H., Mori, K., Miyata, E., Baluta, C., Burrows, D. N., Garmire, G. P., & Chartas,
        G. 2001, ApJ, 554, 496

Wang, L. & Mazzali, P. A. 1992, Nature, 335, 58

Weisskopf, M. C., O'Dell, S. L., & van Speybroeck, L. P. 1996, Proc. SPIE, 2805, 2

Table 1.   List of the *Chandra* Observations of SN 1987A

Observation ID	Date (Age)[a]	Instrument	Exposure (ks)	Source Counts[b]
00124+01387[c]	1999 October 6 (4609)	ACIS-S3 + HETG	116	690
00122	2000 January 17 (4711)	ACIS-S3	9	607
01967	2000 December 7 (5038)	ACIS-S3	99	9031
01044	2001 April 25 (5176)	ACIS-S3	18	1800

[a]Day after the SN explosion in the parentheses.

[b]The source counts were accumulated from a circular region with a radius of $2''$ at $0.3 - 8.0$ keV.
[c]The first observation on 1999 October was split into two sequential observations, which were combined in the analysis.

Table 2.   The $0.5 - 2.0$ keV Flux and Luminosity of SN 1987A from *Chandra* ACIS

Day[a]	Observed Flux $(10^{-13}$ ergs s^{-1} cm$^{-2})$	Luminosity[b] $(10^{34}$ ergs s$^{-1})$
4609	1.53±0.06	6.5
4711	1.57±0.06	6.5
5038	2.23±0.02	9.1
5176	2.44±0.06	10.0

[a]Day after the SN explosion.

[b]Luminosities after removing the absorption.
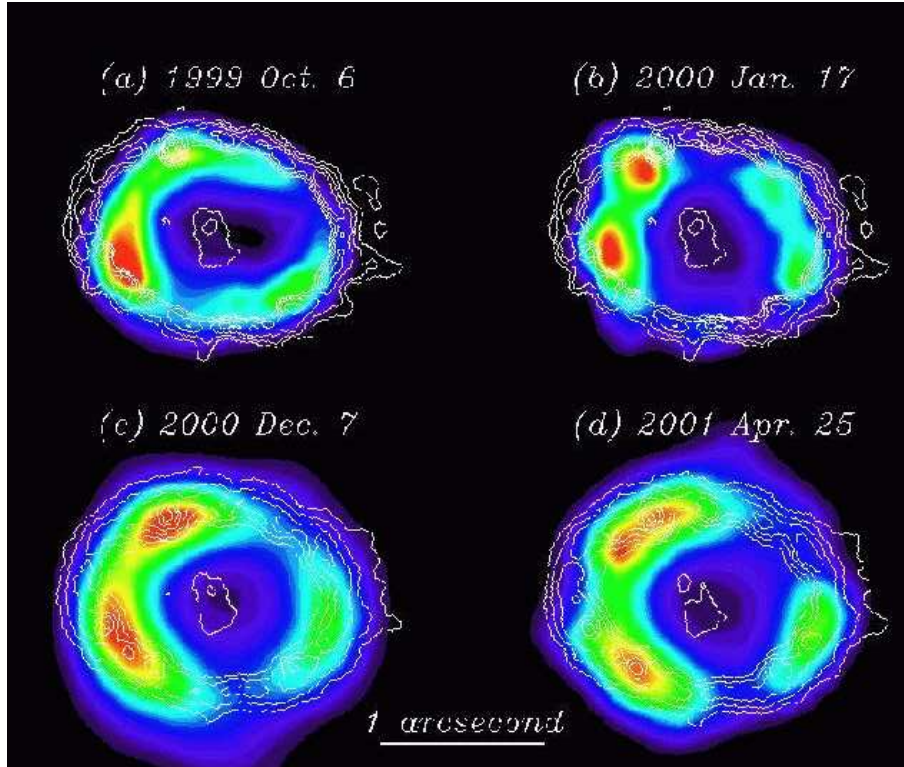
Fig. 1.— ACIS images for SN 1987A. (a) 1999 October 6, (b) 2000 January 17, (c) 2000 December 7, and (d) 2001 April 25. The overlaid contours are from *HST* Hα images as taken 2000 February (a,b), 2000 November (c), and 2001 April (d).
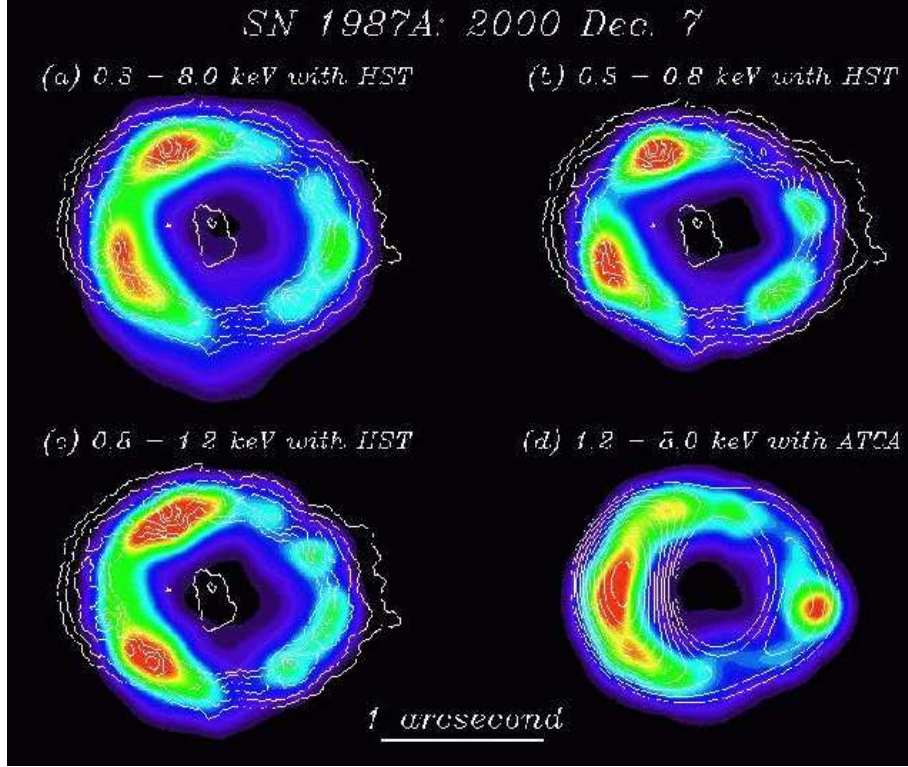
Fig. 2.— ACIS images of SN 1987A as taken on 2000 December 7. (a) $0.3 - 8.0$ keV band, (b) $0.3 - 0.8$ keV, and (c) $0.8 - 1.2$ keV images overlaid with the *HST* contours taken on 2000 November. (d) $1.2 - 8.0$ keV image is overlaid with the *ATCA* 8 GHz contours.
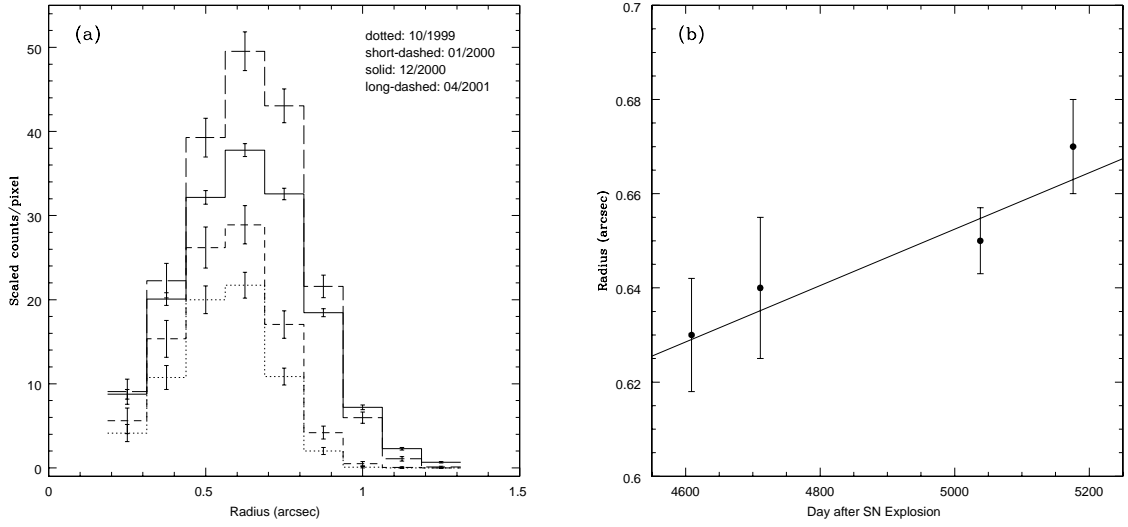
Fig. 3.— Radial profiles of four observations of SN 1987A. (a) is taken from $0.''125$ annular regions over an $\sim1''$ radius around the peak X-ray intensity. (b) is the long-term variation of the mean radius of the X-ray count distribution as obtained with a Gaussian fit. The solid line is the best-fit linear increase rate representing an expansion velocity of ~5200 km s^{-1}.
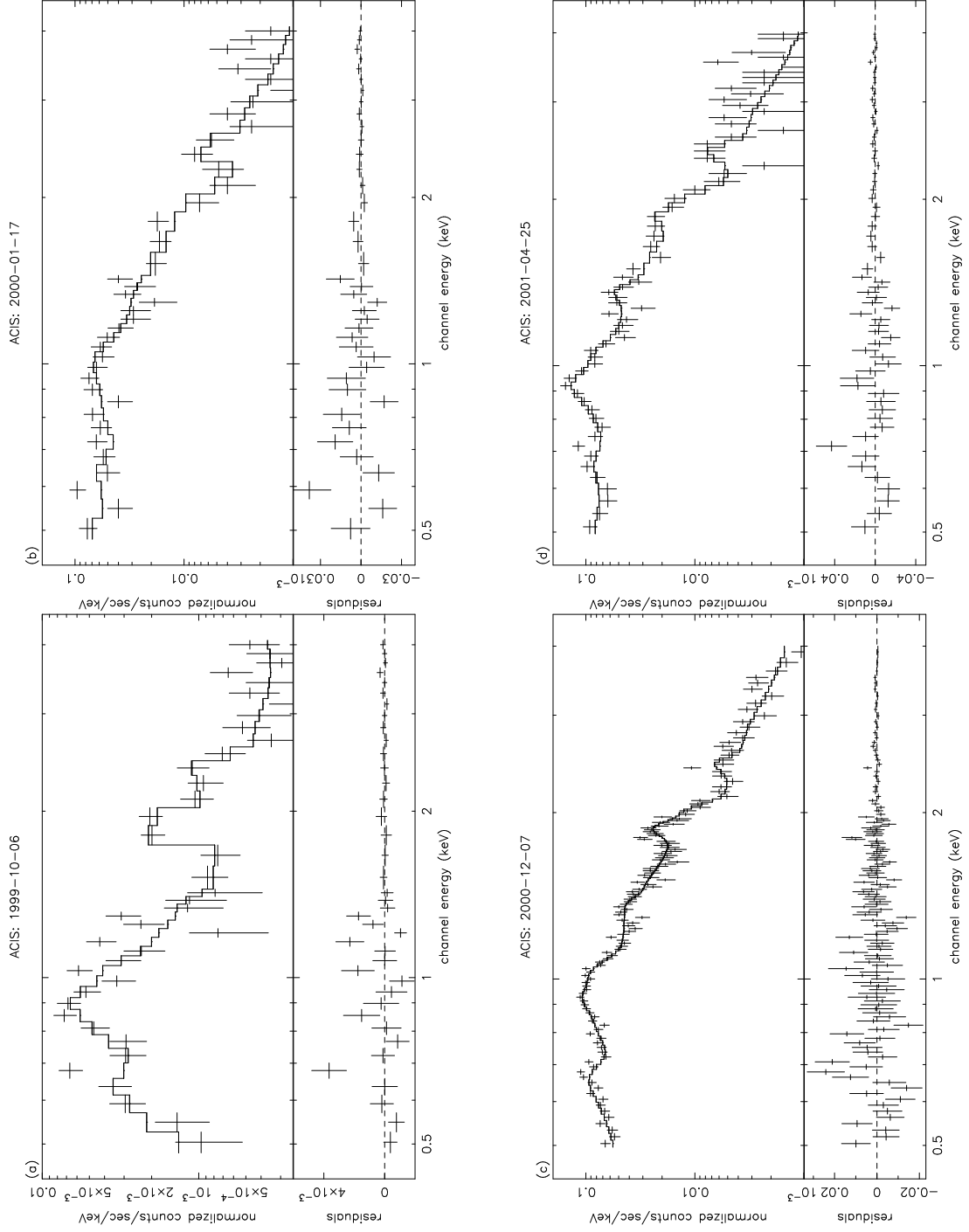
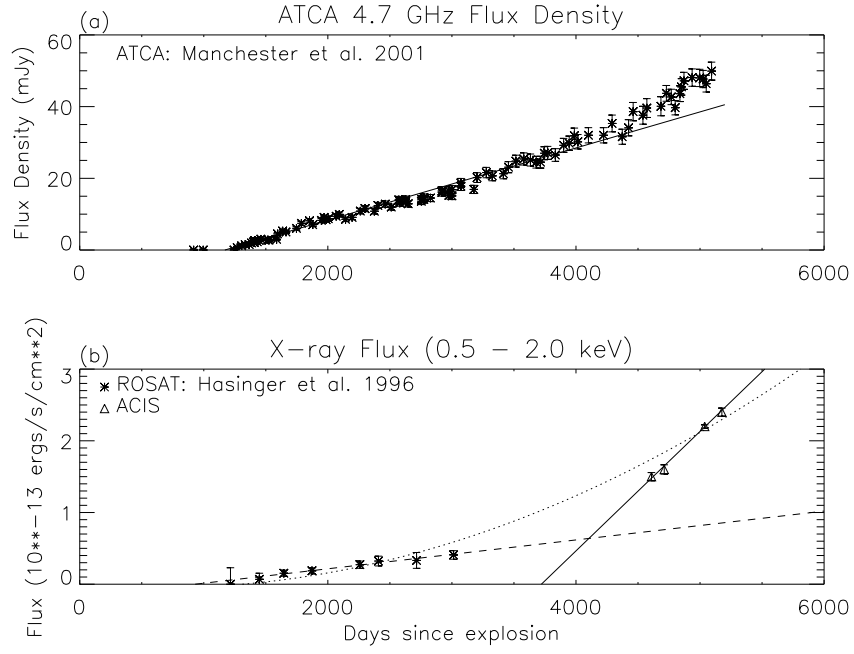Fig. 4.— Spectrum of SN 1987A in the $0.5 - 4.0$ keV band.

Fig. 5.— *Top panel*: (a) The long-term lightcurve of SN 1987A in the 4.7 GHz (ATCA). *Bottom panel*: (b) The long-term X-ray lightcurve of SN 1987A (*ROSAT* and *Chandra* ACIS).